Supplementary Information

General

The multi-reservoir extruder includes the main device as well as an additional electronics box containing several components. The main device measures 330 × 250 × 190 mm. The attached electronics box, which must also sit inside the Prime chamber, measures 150 × 150 × 125 mm. A Power Brick LV-IMS (Delta Tau) is used to control the device. Cables from the device and the electronics box are connected to a 24 V power supply and the Power Brick via a vacuum compatible flange on the Prime chamber. The device and its accessories are controlled through Experimental Physics and Industrial Control System (EPICS) via a graphical user interface.

As stated in the main text, the device comprises three key modules: the reservoir holder, the plunger assembly and the sample interaction region (**Figure 1A**). The device is loaded with up to nine sample-containing reservoir assemblies. These are all described in detail below.

The reservoir assemblies

The sample reservoir assemblies comprise several parts with the key part being the sample reservoir which contains the sample. The additional parts are used to fix the reservoir assemblies within the multi-reservoir extruder and to accommodate extrusion of the sample via a piston actuated mechanically using a stepper motor.

The sample reservoirs (**Figure 1B** and **Supplementary Figure S2**) are analogous to previously published designs (Weierstall, U. *et al* 2014, Botha, S. *et al.* 2015, Shimazu, Y. *et al.* 2019). The sample channel of the sample reservoirs has an inner diameter of 2.2 mm and a total length of 39 mm. This is sealed at one end by compressing a 2.5 mm diameter Teflon ball into the reservoir channel using a custom tool (Supplementary Figure S2). The sample can then be injected from a syringe into the reservoir channel by way of an adaptor to a final volume of approximately 130 µL. The sample reservoir is then sealed with a polyimide coated fused silica capillary needle (75 µm ID, 363 µm OD) Polymicro Technologies™, Molex®), fitted with a 12 mm PEEK tubing sleeve (0.15 in ID, 1/16 in OD) and a LT-100X LiteTouch® Ferrule (IDEX) assembly. This capillary needle assembly is fixed in place onto the reservoir channel using a nut, tightened to 2.0 Nm using a torque wrench.

The additional parts of the sample reservoir assembly include a plunger, a brass sheath, a spring and a bayonet sleeve. The plunger sits inside the brass sheath and the spring and bayonet sleeve are loaded onto the outside of this brass sheath. The brass sheath can then be screwed into the sample reservoir via a threaded connection bringing these additional parts together with the sample reservoir to form the complete sample reservoir assembly. Once assembled, the head of the plunger is able to contact the Teflon ball within the reservoir channel at the back of the sample. The tail of the plunger has a flat surface which is accessible to the plunger assembly through an opening in the brass sheath. It is this contact which permits sample extrusion. The function of the spring and bayonet sleeve is to hold the sample reservoir assembly in place within the reservoir holder drum.

The reservoir holder

The reservoir holder can hold up to nine reservoirs and is responsible for selecting the desired reservoir, readying it to be delivered to the sample interaction region. A belt drive mechanism powers the reservoir holder drum. The drum moves unidirectionally and is actuated by a stepper motor (ST4118M906-B, Nanotec) equipped with an incremental encoder on its motor shaft (NOE2-05-K14 (5MM), Nanotec). A forked photoelectric sensor (PM-F45, Panasonic) is used to identify a reference position and align the reservoir holder drum. This is achieved via detection of a reference marker mounted on the moving part of the drum.

The reservoir holder drum was 3D-printed from CL 20ES stainless steel (Kyburz Feinmechanik AG) in order to facilitate the incorporation of liquid feedthrough channels surrounding each of the nine reservoir positions (Supplementary Figure S1). The liquid feed-through channels can be connected to a circulating chiller (Julabo FN25 EH) in order to stabilise the temperature of the reservoir holder drum at 20ºC for peak stability of LCP samples. It was possible to reach sample reservoir temperatures of 12ºC to 45ºC inclusive, as measured using a thermocouple attached to a sample reservoir mounted in the reservoir holder (Supplementary Figure S2A).

The sample interaction region

The sample interaction region sits on a stationary mount and comprises: 1) a fibre optical sensor, to detect the incoming sample capillary during sample selection and loading, 2) a guiding aperture to direct and align the incoming capillary needle, 3) a gas aperture mount, to house the ceramic gas aperture and to connect to the incoming sheath gas supply, 4) a YAG crystal in the plane of the jet, for beam diagnostic purposes, 5) a tip cleaner, to remove built up debris and sample from the capillary tip and 6) a ‘catcher’, connected to a vacuum pump, to collect extruded sample and stabilise the sample jet (Supplementary figure S3).

To position the tip of the capillary at the sample interaction region, the reservoir holder containing loaded reservoirs and the plunger assembly are translated together by way of a linear stage. This linear stage has built in limit switches and an incremental encoder (MTM-120, Owis). In short, after the selected reservoir has been rotated into position by the reservoir holder assembly, the linear stage moves it forward towards the sample interaction region. This motion threads the capillary needle into the sample interaction region, ready for extrusion to take place. It is also responsible for retracting the needle and reservoir once the sample reservoir is empty.

In order to accommodate variable capillary needle lengths – as these are produced manually and can have millimetres of variation in length – a fibre optical sensor (LL3-DZ02, GLL170-P332, Sick) is mounted in front of the guiding aperture at the entrance to the sample interaction region. As the capillary needle tip moves over the sensor, a reflection of the emitted light (wavelength, 632 nm) occurs and, once detected, provides a homing reference for the motion of the capillary needle towards the sample interaction region. The light from the sensor is turned off once this procedure has taken place to avoid light contamination of the sample. The distance between this sensor and the opening of the ceramic gas aperture (ref, Arizona State University. Centre for Biological Physics) is constant and during these experiments was calibrated as 26.5 mm. The reservoir and capillary needle could then be driven this distance automatically. This positioned the tip of the capillary needle in a

reproducible but slightly retracted position with respect to the ceramic gas aperture opening. At this point, manual positioning of the capillary needle using the linear stage in fine, 50-100 μm steps could be carried out. This allowed for accurate and reproducible control of the position of the capillary needle and thus, viscous jet, with respect to the concentric gas flow from the ceramic aperture. This position could also be optimised during extrusion of the sample to flexibly permit maximum jet stability.

A detachable tip cleaner fitted with a disposable sponge was magnetically mounted below the sample interaction region onto a linear piezo-stage (SLC-1720, Smaract). The capillary tip and ceramic gas aperture could thus be cleaned without the need to break the vacuum environment of the Prime chamber during operation. Cleaning of the tip was also performed once a sample reservoir was depleted to ensure that residual sample present on the capillary tip was not deposited inside the stationary ceramic gas aperture upon retraction of the capillary needle during the automated sample reservoir exchange sequence.

A 'catcher' was magnetically mounted downstream of the capillary needle on a linear piezo-stage (SLC-1720, Smaract) and was connected to a vacuum pump. The remote motion of the catcher permitted on-the-fly stabilisation and tuning of the sample jet stability. The catcher had a conical opening with diameter 9.3 mm feeding into a cylindrical body with diameter 19 mm and length 60 mm. Using a dry scroll vacuum pump (nXDS 10iC, New Edwards) fitted with a gas flow meter (Vögtlin), a vacuum was applied to the catcher. The catcher was fitted with a removable mesh filter and both the catcher and filter could be removed and cleaned during sample reservoir exchanges.

The plunger assembly

The plunger assembly is responsible for extruding the sample at a desired flow rate and velocity (Supplementary Figure S4). A stepper motor (SCA2018M0804-A, Nanotec) and gear box (GPLE22-2S-9, Nanotec) are connected via a belt drive to a plunger actuator. The motor drives this plunger actuator into the back of the plunger of a sample reservoir assembly. The plunger is then pushed forward, extruding the sample from the sample reservoir through the capillary needle at a defined velocity.

During data collection, the plunger actuator generally moves at velocities in the low μm/s range. However, a second, faster speed (500 μm/s) is used during sample exchange to reduce the downtime between samples. The issue is that when the plunger actuator moves the plunger with high speed into the sample, a fast pressure build up can result in sample loss and/or potential damage to the capillary needle or ceramic gas aperture. To avoid this rapid pressure change, a load cell (Subminiature load cell 8413, Burster) monitors the applied force of the plunger actuator and as soon as the force exceeds a defined value, the plunger motor is stopped and the plunger actuator retracts 500 μm from its current position. When the user is ready to begin sample extrusion for data collection, the motor can be restarted at the desired reduced velocity. The load cell and its in-line amplifier provide a 0 - 10 V signal, which correspond to 0 - 200 N. The signal is processed by a threshold relay, which can be adjusted by a potentiometer.

Positive and negative limit switches (IFFM 08P37A6/L, Baumer) sit at each end of the 40 mm travel range of the plunger actuator. As well as limiting the motion of the plunger actuator, these permit an accurate feedback of the amount of sample remaining at any given point during sample extrusion. The limit switches, combined with the continuous feedback of the force exerted on the load cell during sample extrusion mean that blockages of the capillary needle can be easily distinguished from the sample reservoir being empty.

Temperature control tests

Temperature control tests of the multi-reservoir assembly were carried outside the Alvra Prime chamber at atmospheric pressure and ambient temperature (23ºC). Acting as a thermocouple, DT-421 Series Silicon Diode was used to measure the temperature of an empty reservoir with respect to the demand temperature of the circulating cooling fluid within the reservoir holder drum. The thermocouple was connected to a single reservoir via a vacuum feedthrough. The thermocpule was connected to LakeShore Temperature control unit (Model 331) which was used to automatically log the temperature. The reservoir was then placed inside one of the reservoir holder drum positions analogous to how it would be during sample extrusion.

The temperature of the circulating fluid within the reservoir holder drum was set using a Julabo F25-EH circulator filled with Thermal-G (Julabo). The temperature of the thermocouple attached to the reservoir was recorded manually while setting the circulator temperature between 5ºC and 45ºC in 5 degree increments. The temperature of the thermocouple at each set point was left to stabilize such that the temperature did not change over a timescale of 10 minutes or longer.

A standard curve of the demand temperature set on the circulator versus the feedback from the thermocouple attached to the reservoir was calculated (Figure 1C). When increasing the temperature in 5 degree increments, the circulator took approximately 7 minutes to stabilize at the demand temperature (to 0.25ºC precision). The corresponding change of the thermocouple took up to 20 minutes (to 1ºC precision). Temperatures below 5ºC were not attempted due a risk of ice or condensation on the circulator lines and multi-reservoir assembly. Temperatures above 45ºC were avoided due to the operating temperature limits of the motors of the multi-reservoir assembly.

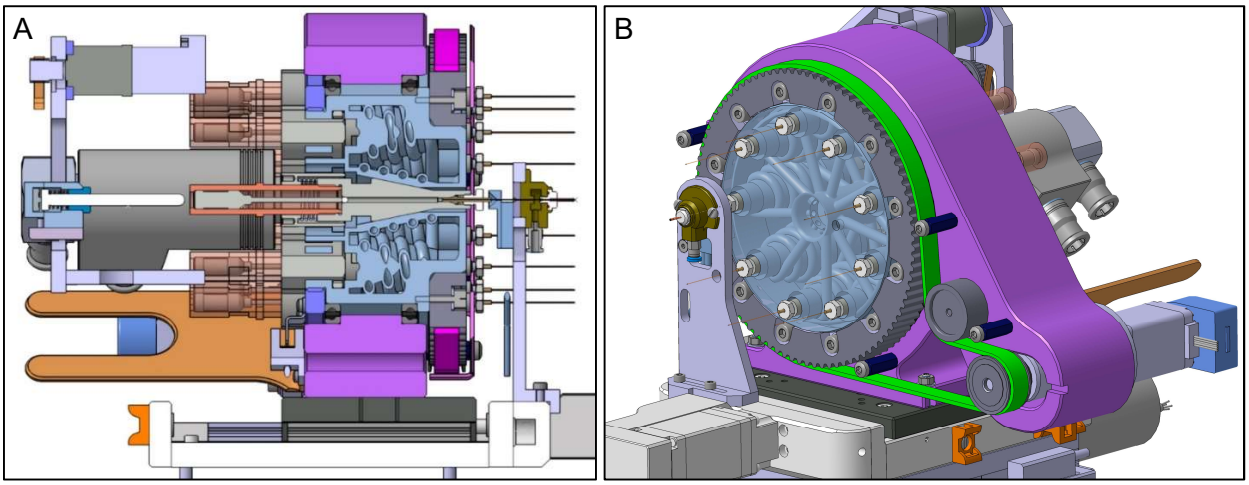

Supplementary figure S1. Liquid feedthrough channels of the reservoir holder drum. Panel A shows a vertical cut through of the drum and a reservoir assembly. Panel B shows an oblique view device with the reservoir holder drum in a transparent material so that the arrangement of the liquid feedthrough channels is visible within the 3D printed steel.

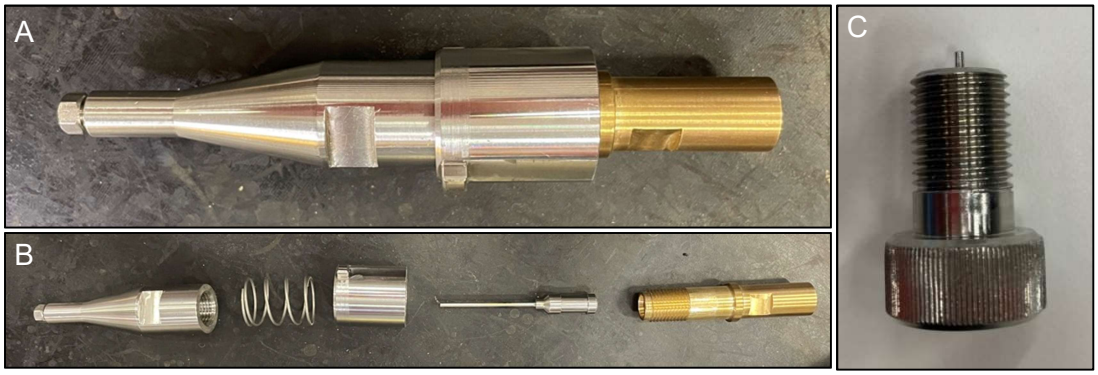

Supplementary figure S2. The reservoir assembly and tool for Teflon ball insertion. Panel A shows the assembled reservoir assembly body and panel B contains the components of the reservoir assembly in an exploded view. The tool made in house for reliable insertion of the Teflon ball within the reservoir channel.

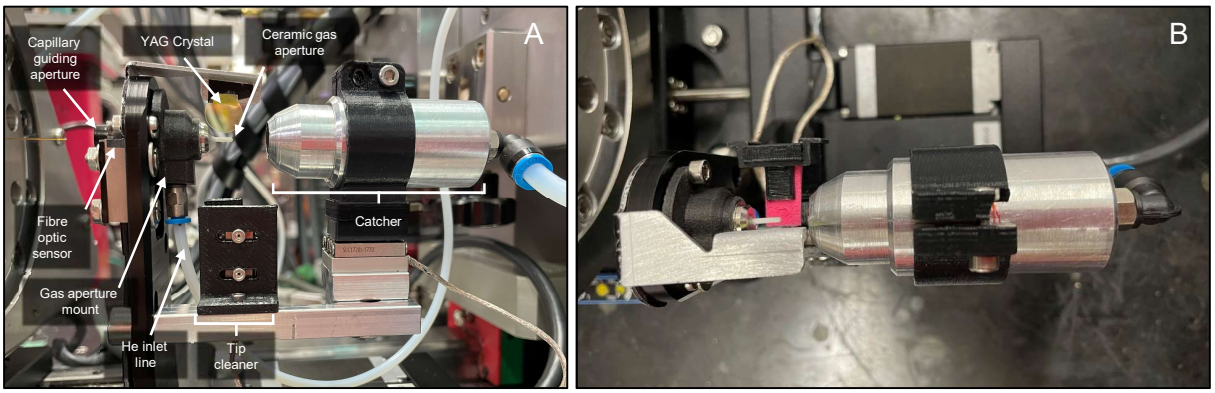

Supplementary figure S3. The sample interaction region. Panel A shows a side on view with all features annotated. In this panel the arm of the tip cleaner is removed so that other elements are clearly visible. Panel B shows a top view with the arm of the tip cleaner in place with the pink sponge clearly visible.

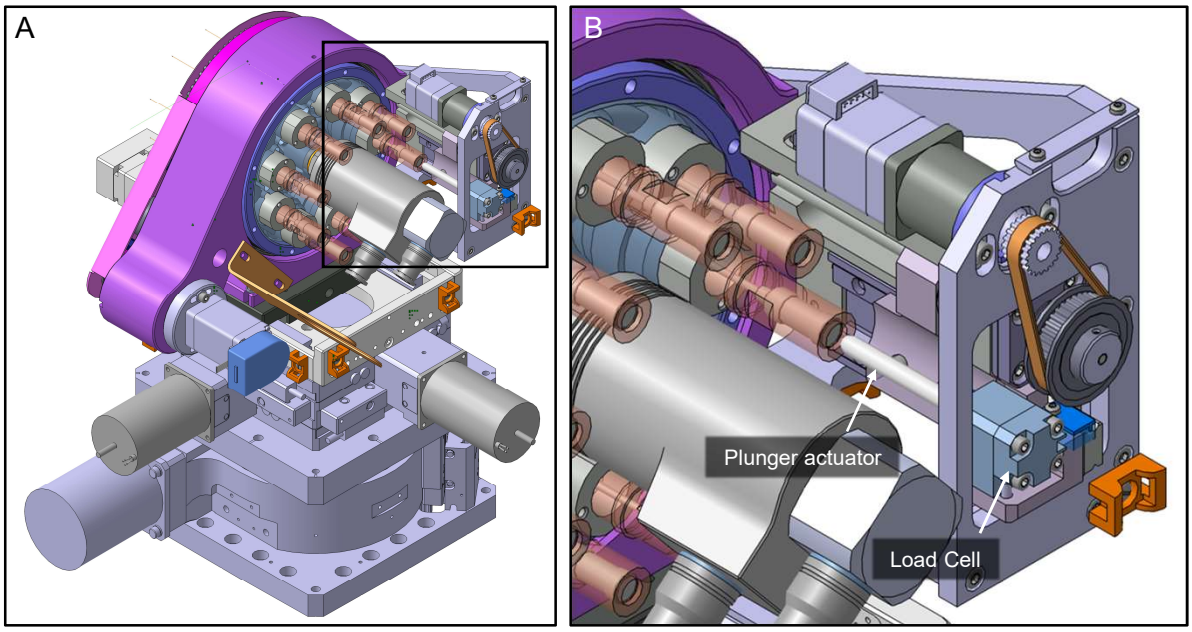

Supplementary figure S4. Detailed view of the plunger assembly. Panel A shows the plunger assembly with inset square magnified in panel B. The plunger actuator, which contacts the plunger within the reservoir assembly and controls extrusion is indicated. The load cell registers the force exerted on the plunger rod and provides a measure of pressure exerted on the plunger rod.

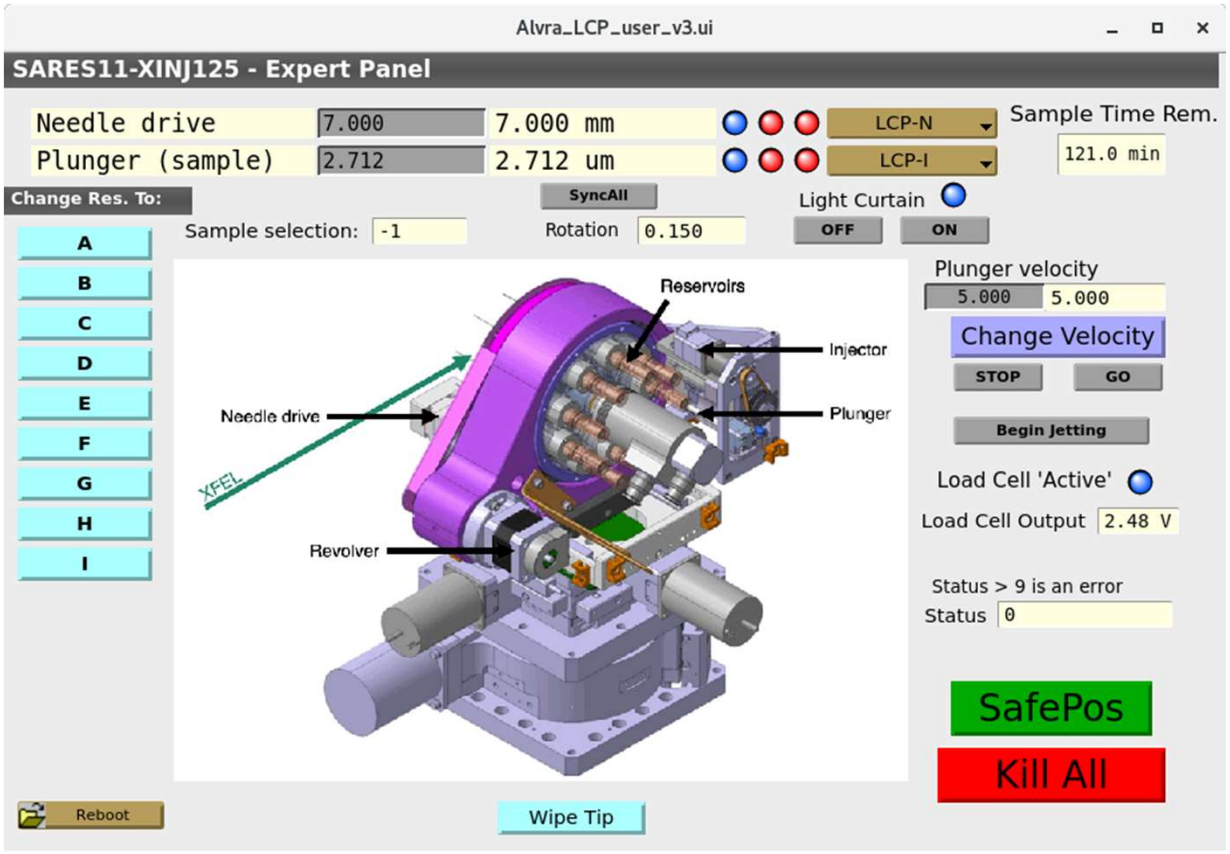

Supplementary figure S5. Graphical user interface for the multi-reservoir high viscosity extruder. Reservoir positions A-H can be chosen with the blue buttons on the left of the panel – these initiate the automatic loading sequence of the chosen reservoir. The light curtain used for positional feedback of the capillary tip during the loading sequence can be toggled off once the reservoir assembly is in place in order to avoid light contamination of the sample. The 'Load Cell Output' readback value represents the force exerted on the plunger actuator as a voltage – the 'Load Cell 'Active'' indicator turns blue when the plunger is in contact with the sample and grey in other instances. The desired plunger velocity in µm/s is typed in by the user and then jetting is initiated by clicking the 'Begin Jetting' button. The 'Wipe Tip' button triggers an automated sequence to clean debris from the tip of the capillary needle using a sponge.

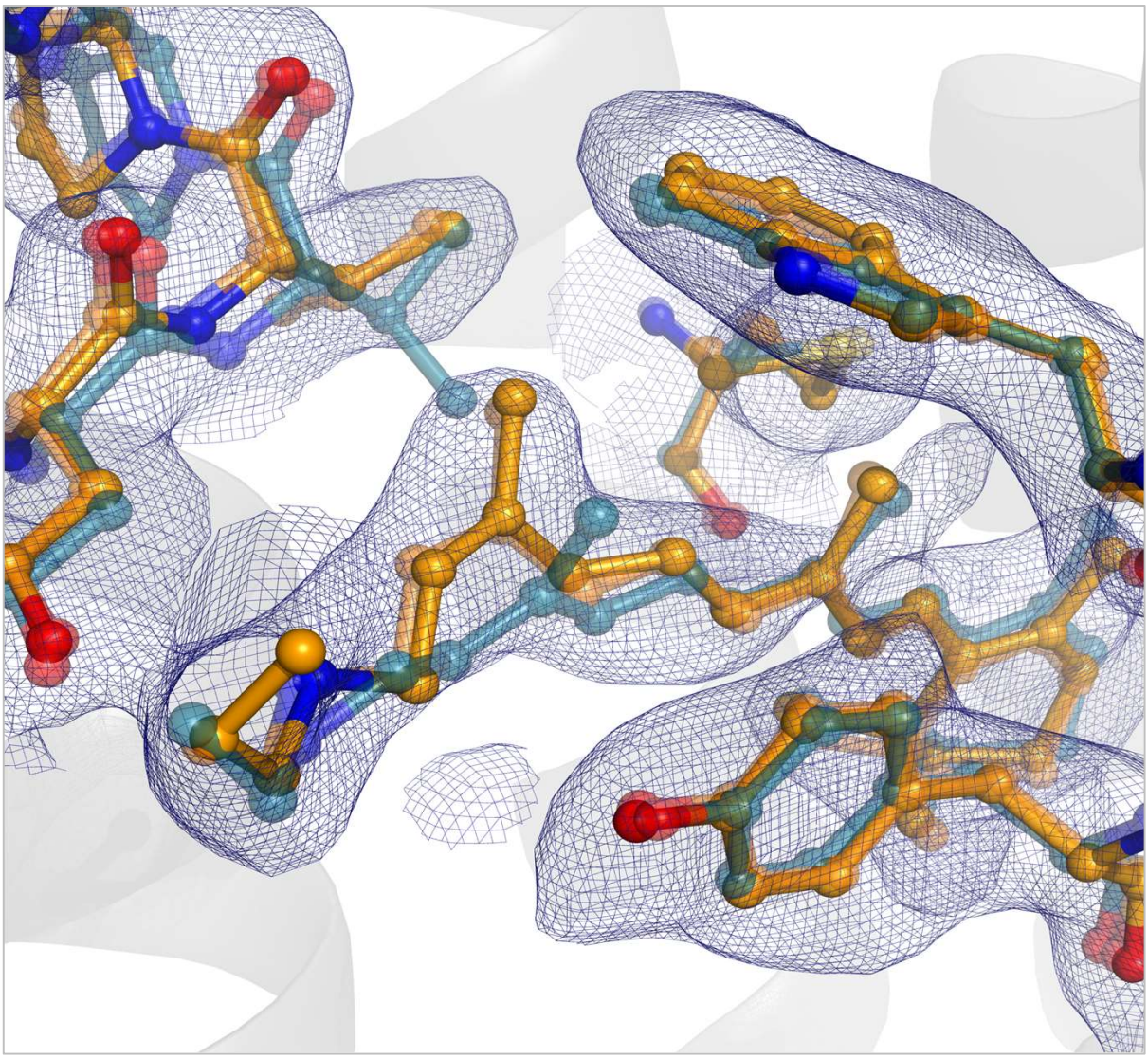

Supplementary figure S6. KR2 extrapolated map, $2F_{ext}–F_c$ at 19% activation level for 1 μs time delay presented around the retinal pocket. Yellow model depicts the refined KR2 structure in extrapolated map and blue and orange transparent models represent dark 6TK6 and 1 ms light 6TK2 structures. Electron density shown at sigma level of 1.0.

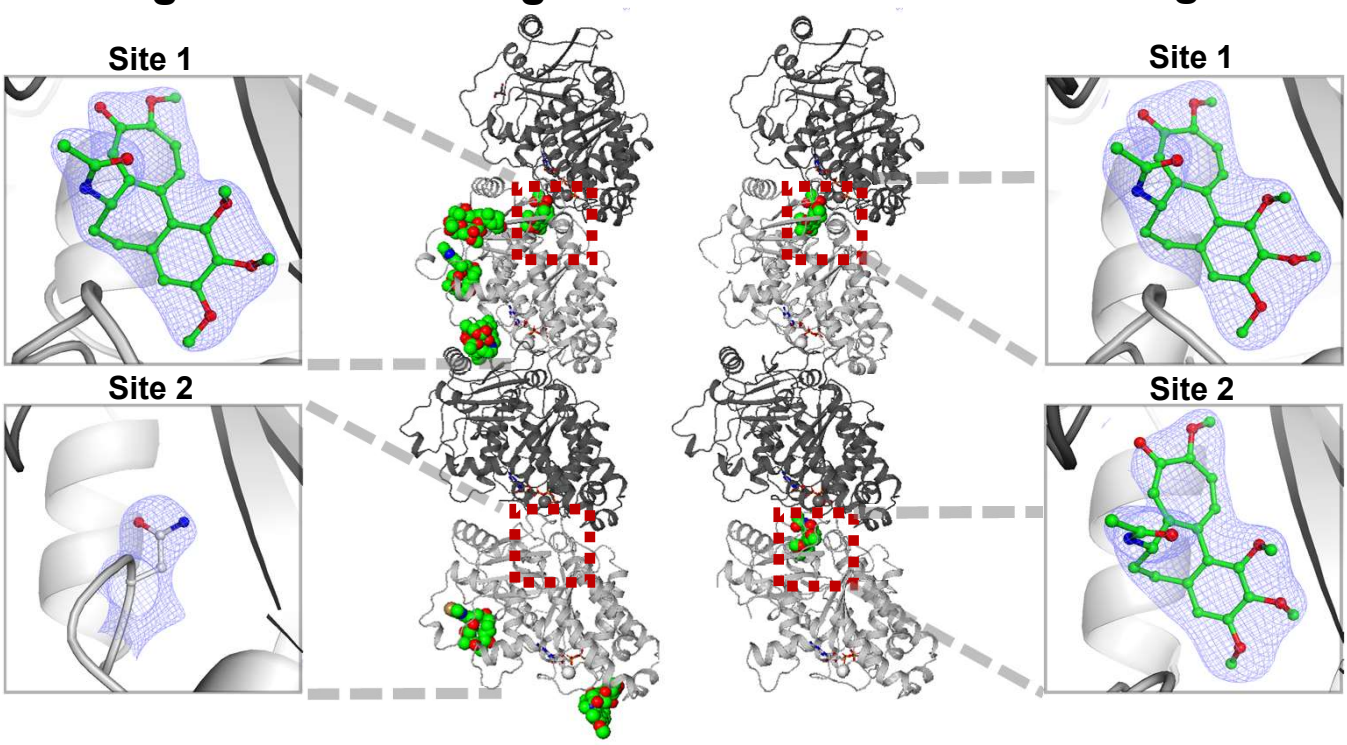

Supplementary figure S7. Global effects of multiple ligand binding. (A) Cocktail of ligands facilitates the exploration of global effects whereby simultaneous ligand mixing might influence affinity levels at different binding sites as compared to (B) mixing with a single compound. For both soaks identical concentration of Colchicine ligand were used. Electron denisty ($2F_o$-F_c) maps are shown at sigma level of 1.0. The apo protein (A, site 2) is indicated by the flipped-in residue ASN247.

Site 1 – high occupancy binding

Standard omit maps

5000 patterns

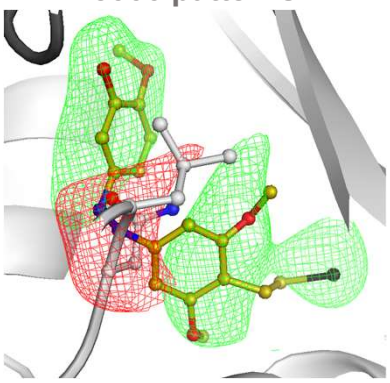

4000 patterns

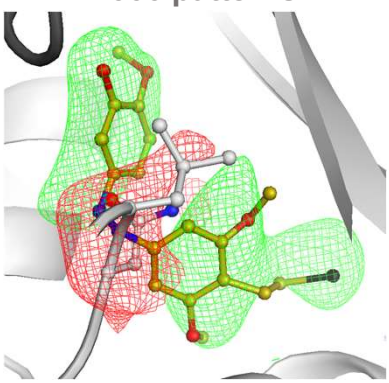

3000 patterns

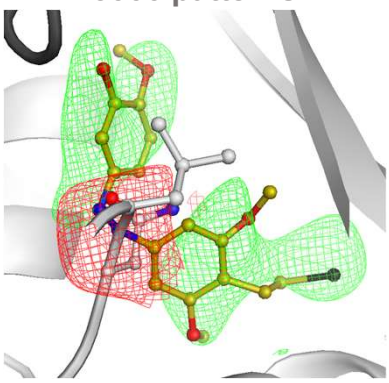

2000 patterns

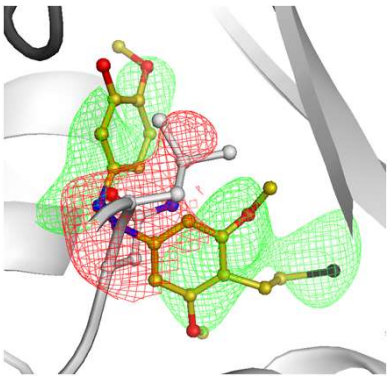

1000 patterns

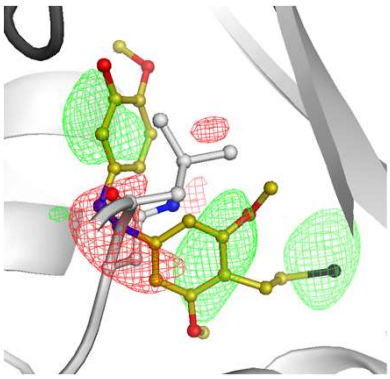

500 patterns

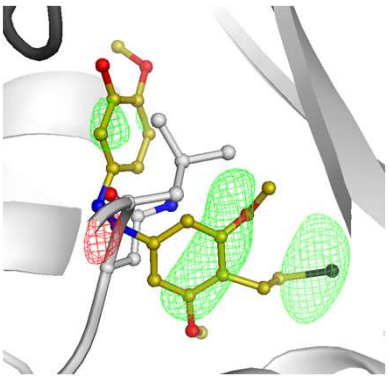

Isomorphous difference density maps

5000 patterns

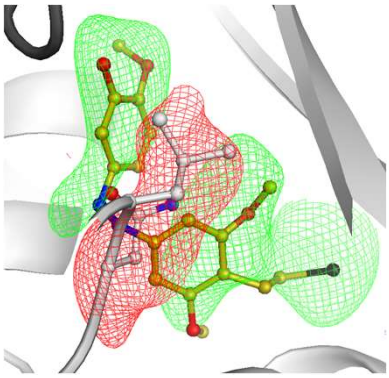

4000 patterns

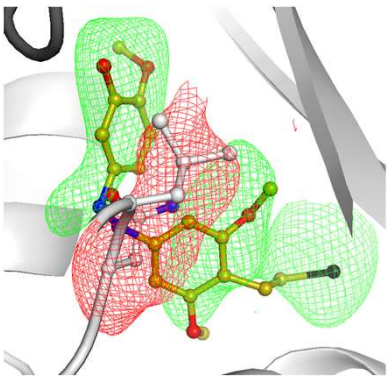

3000 patterns

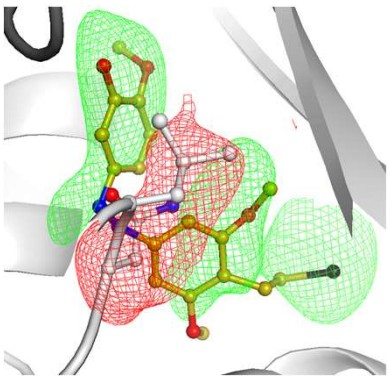

2000 patterns

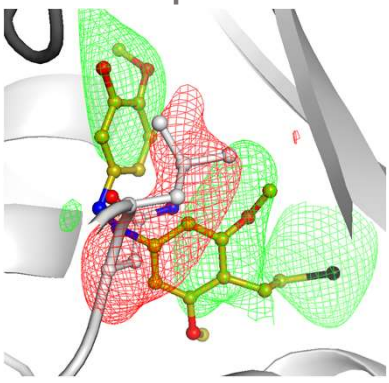

1000 patterns

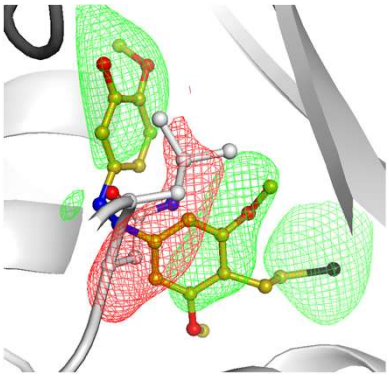

500 patterns

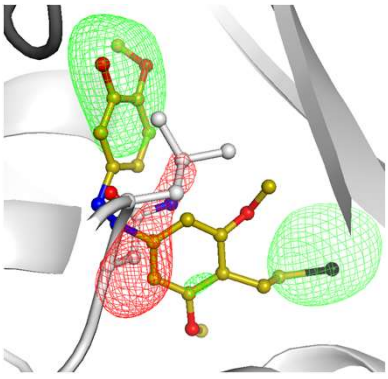

Supplementary figure S8. Titration series of minimal amount of data required to reliably detect SolQ2Br binding within the high occupancy binding site 1. Comparison between standard omit (F_o-F_c) maps against apo protein state and isomorphous difference density (F_o-F_c) maps. The SolQ2Br structure is overlaid for better illustration. All maps are shown at a sigma level of 1.0. Positive difference density is shown in green, negative difference density in red.

Site 2 – low occupancy binding

Standard omit maps

5000 patterns

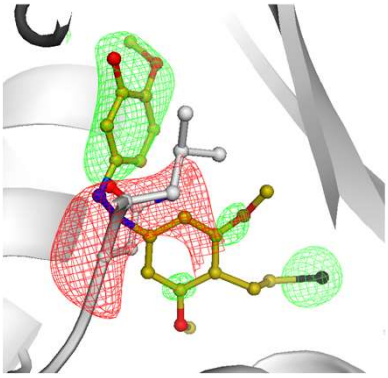

4000 patterns

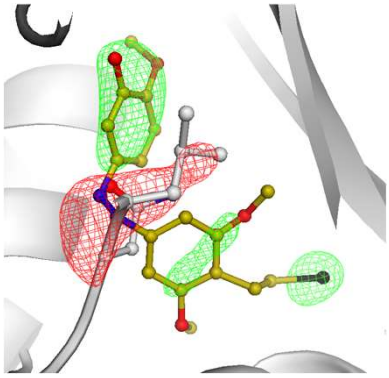

3000 patterns

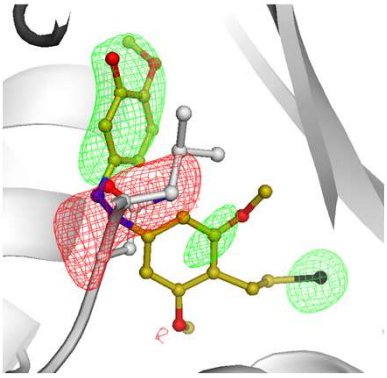

2000 patterns

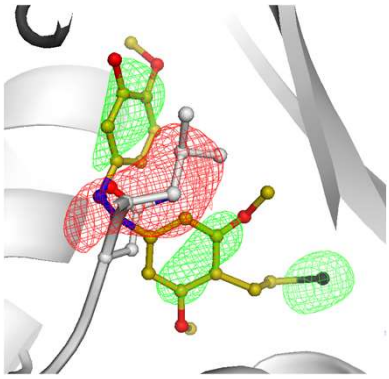

1000 patterns

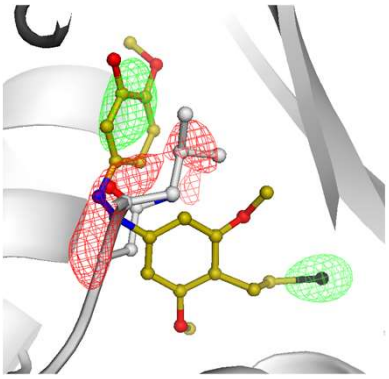

500 patterns

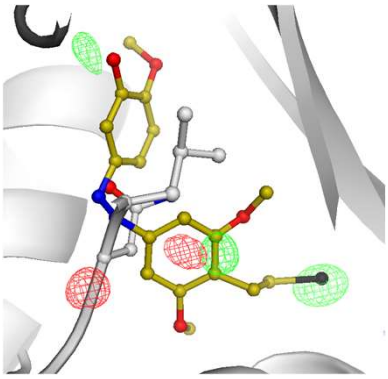

Isomorphous difference density maps

5000 patterns

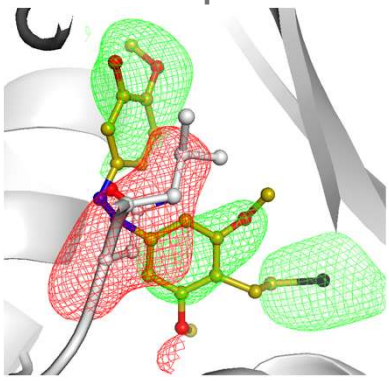

4000 patterns

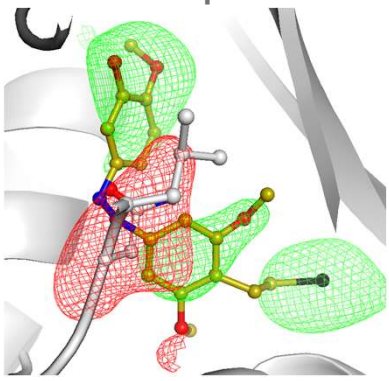

3000 patterns

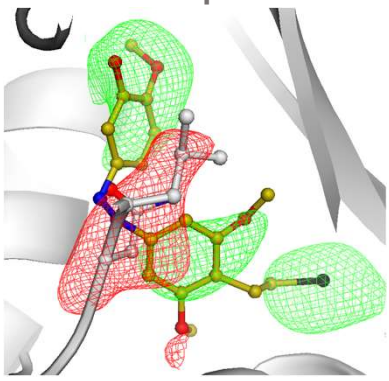

2000 patterns

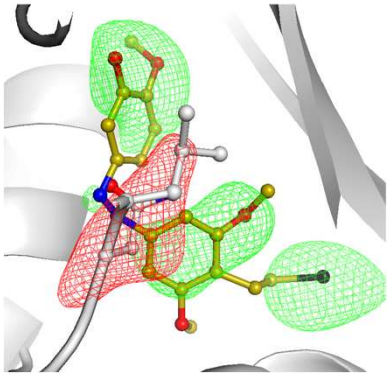

1000 patterns

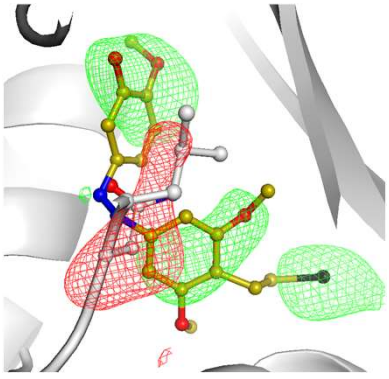

500 patterns

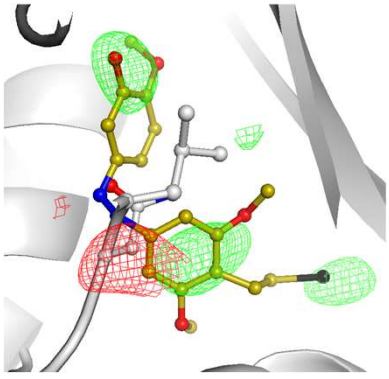

Supplementary figure S9. Supplementary figure S8. Titration series of minimal amount of data required to reliably detect SolQ2Br binding within the low occupancy binding site 2. Comparison between standard omit (F_o-F_c) maps against apo protein state and isomorphous difference density (F_o-F_c) maps. The SolQ2Br structure is overlaid for better illustration. All maps are shown at a sigma level of 1.0. Positive difference density is shown in green, negative difference density in red.

Plunger Speed (µm/s)	Measured speed (µm/s)	Calculated Speed (µm/s)	Ratio calulcated/actual
1	916	860	93.8%
2	1619	1721	106.3%
5	4647	4302	92.6%
10	8439	8604	102.0%
15	14568	12907	88.6%
20	18979	17208	90.7%
25	26490	21511	81.2%
30	30960	25813	83.4%

Supplementary table T1: Sample extrusion speeds obtained from fast camera recordings. The calculated speed was estimated by solving volumetric flow rate equation.